ELSEVIER

Applied Catalysis A: General 211 (2001) 19–30

APPLIED CATALYSIS A: GENERAL

www.elsevier.com/locate/apcata

An XPS study of the dispersion of MoO_3 on TiO_2–ZrO_2, TiO_2–SiO_2, TiO_2–Al_2O_3, SiO_2–ZrO_2, and SiO_2–TiO_2–ZrO_2 mixed oxides

Benjaram M. Reddy [a,*], Biswajit Chowdhury [a], Panagiotis G. Smirniotis [b,1]

[a] *Inorganic Chemistry Division, Indian Institute of Chemical Technology, Hyderabad 500007, India*
[b] *Chemical Engineering Department, University of Cincinnati, Cincinnati, OH 45221-0171, USA*

Received 11 August 2000; received in revised form 19 October 2000; accepted 19 October 2000

Abstract

X-ray photoelectron spectroscopy technique was employed to characterize TiO_2–ZrO_2, TiO_2–SiO_2, TiO_2–Al_2O_3, SiO_2–ZrO_2, and SiO_2–TiO_2–ZrO_2 mixed oxide supported MoO_3 catalysts. The investigated mixed oxide supports are obtained by a homogeneous coprecipitation method using urea as hydrolyzing agent. Molybdena (12 wt.%) was impregnated over these calcined (773 K) mixed oxide supports by a wet impregnation method from aqueous ammonium heptamolybdate solution. The XPS binding energy (BE) values of all the metals in the mixed oxide supports as well as Mo-containing catalysts are found to shift from the values of the individual metal component oxides. The shift in BE suggests that the Zr in TiO_2–ZrO_2 and Ti in TiO_2–Al_2O_3 acquire more negative charge after doping with MoO_3 on these supports. The observed BE shifts, due to variation in the lattice potential, are explained in terms of Kung's model. The XPS atomic intensity ratio measurements show that the interaction between Mo and Al is strong and the dispersion of molybdena is more on Al_2O_3 portion of the TiO_2–Al_2O_3 mixed oxide. In the case of MoO_3/TiO_2–ZrO_2 and MoO_3/SiO_2–TiO_2–ZrO_2 samples, the Mo:Ti and Mo:Zr ratios show that the Ti^{4+} and Zr^{4+} both contribute equally in the dispersion of molybdenum on these corresponding mixed oxides. The FWHM values indicate the presence of different Mo(VI) species on TiO_2–Al_2O_3, and a homogeneous distribution on TiO_2–ZrO_2 and TiO_2–SiO_2 mixed oxide surfaces.

Keywords: Molybdenum oxide; Mixed oxides; TiO_2–ZrO_2; TiO_2–SiO_2; TiO_2–Al_2O_3; SiO_2–ZrO_2; SiO_2–TiO_2–ZrO_2; Dispersion; XPS

1. Introduction

Supported molybdenum oxide catalysts are widely used in various catalytic processes [1–5]. These catalysts are normally obtained by impregnating the catalytically active molybdenum oxide species on an inorganic oxide support (Al_2O_3, SiO_2, TiO_2, and ZrO_2) for the purpose of (1) increasing the catalytic activity and selectivity, (2) extending the life of the catalysts, and (3) augmenting the mechanical strength of the catalysts. It is well established in the literature that the structure of the dispersed molybdenum species is closely related to the nature of the specific oxide support, the loading amount, the preparation procedure, and the calcination temperature [1,5]. It is also well known that the type of support plays an important role on the catalytic properties and for a given reaction the activity and selectivity of the catalyst can be improved by the use of an appropriate support oxide [4].

* Corresponding author. Fax: +91-40-7173387.
E-mail addresses: bmreddy@iict.ap.nic.in (B.M. Reddy), panagiotis.smirniotis@uc.edu (P.G. Smirniotis).
[1] Co-corresponding author. Fax: +1-513-556-3473.

0926-860X/01/$ – see front matter
PII: S0926-860X(00)00834-6

Previous research has highlighted the use of alumina, silica, titania, and zirconia as supports for molybdena based catalysts for hydroprocessing applications [1,6–9]. High activity and selectivity is usually provided to a catalyst by the compounding of two or more functionalities on the same material. To devise a better hydrotreating catalyst two functions namely, hydrogenolysis activity and acidity should be combined. The need for new and improved hydroprocessing catalysts with different distribution of catalytic functionalities has increasingly inspired the research in the use of mixed oxides as supports. Various mixed oxides such as TiO_2–SiO_2, TiO_2–ZrO_2, SiO_2–ZrO_2, TiO_2–Al_2O_3 have already been attempted in a number of industrially important catalytic reactions such as dehydrocyclization of *n*-paraffins to aromatics [10], isomerization of butanes [11], dehydration of cyclohexanol [12], selective catalytic reduction of NO_x, etc. [13,14].

Several models have been proposed to explain the dispersed state of molybdena on different single oxide supports [1–5,15–17]. These models can be divided mainly into two categories: the first model suggests that under appropriate conditions a monolayer of the dispersed ionic compound is formed on the surface of the support, and the second proposes that instead of forming an overlapping monolayer, the dispersed metal cations are incorporated into the surface vacant sites of the support with their accompanying anions staying on top of them for charge compensation. Among various spectroscopic methods available for characterization of these catalysts [4,16,18,19], the X-ray photoelectron spectroscopy (XPS or ESCA), because of its high surface sensitivity (probing depth ca. 2 nm), has been considered as one of the best techniques for studying the dispersion of MoO_3 on various supports and to gain knowledge on the type of interaction involved between the active metal species and the supporting oxide. Thus, XPS has been utilized for the general characterization of Mo-containing catalysts and also to study the dispersion of Mo on different supports by various groups [20–27]. However, in most cases only γ-Al_2O_3 has been used as the support material. The primary goal of this study was to examine the dispersion and nature of Mo-oxide species, as observed from XPS measurements, on different mixed oxide supports for the first time. The various mixed oxide supports TiO_2–ZrO_2, TiO_2–SiO_2, TiO_2–Al_2O_3, SiO_2–ZrO_2, and SiO_2–TiO_2–ZrO_2 used in this investigation are obtained by a homogeneous coprecipitation method and were deposited with MoO_3 by adopting a wet impregnation technique.

2. Experimental section

2.1. Catalyst preparation

All the mixed oxide supports used in this investigation are prepared by a homogeneous coprecipitation method using urea as hydrolyzing agent [28]. The appropriate amount of cold $TiCl_4$ (Fluka, AR grade) was initially digested in cold concentrated HCl and then diluted with doubly distilled water. To this aqueous solution the required quantity of Na_2SiO_3 (AR grade, Loba Chemie) or $ZrOCl_2{\cdot}8H_2O$ (AR grade, Loba Chemie) or $NaAlO_2$ (AR grade, Loba Chemie), dissolved separately in deionized water, was added. An excess urea solid (AR grade, Loba Chemie) was also added to this mixture solution for better control of pH and heated to 368 K with vigorous stirring. After about 6 h of heating a white precipitate was gradually formed in the solution as the urea decomposition progressed to a certain extent. The precipitate was heated for 6 more hours to facilitate aging. The precipitate thus obtained was thoroughly washed with deionized water until no chloride ions could be detected with $AgNO_3$ in the filtrate. The obtained cake was then oven dried at 393 K for 16 h. In order to remove sodium ions the oven dried precipitates were washed with aqueous ammonium nitrate (Loba Chemie, GR grade) solution (5%) and again with hot distilled water for several times. The pure chloride free hydroxide coprecipitates thus obtained were dried once again at 393 K for 16 h and finally calcined at 773 K for 6 h in open-air atmosphere.

Molybdena (12 wt.% nominal) was deposited on various mixed oxide supports by adopting a wet impregnation method. To impregnate MoO_3 the calculated amount of ammonium heptamolybdate (J T Baker, England, AR grade) was dissolved in doubly distilled water and a few drops of dilute NH_4OH was added to make the solution clear and to keep the pH constant (pH = 8). Finely powdered calcined (773 K) supports were then added to this solution and the excess water was evaporated on a water-bath with continuous stirring. The resultant solid was then

dried at 383 K for 12 h and calcined at 773 K for 5 h in the flow of oxygen (40 $cm^3\,min^{-1}$). The rate of heating (as well as cooling) was always maintained at 10 $K\,min^{-1}$. In the text all the catalysts containing 12 wt.% (nominal) MoO_3 were labeled as MTZ (MoO_3/TiO_2–ZrO_2); MTS (MoO_3/TiO_2–SiO_2); MTA (MoO_3/TiO_2–Al_2O_3); MSZ (MoO_3/SiO_2–ZrO_2) and MSTZ (MoO_3/SiO_2–TiO_2–ZrO_2), and the pure supports as TZ (TiO_2–ZrO_2), TS (TiO_2–SiO_2), TA (TiO_2–Al_2O_3), SZ (SiO_2–ZrO_2) and STZ (SiO_2–TiO_2–ZrO_2), respectively, for the sake of convenience in discussing the results.

2.2. XRD and BET surface area

X-ray diffraction analysis was performed on a Siemens D-5000 diffractometer by using Cu Kα radiation source and Scintillation Counter detector. The XRD phases present in the samples were identified with the help of ASTM Powder Data Files. The BET surface area of the samples was determined by N_2 physisorption at 77 K by taking 0.162 nm^2 as the area of cross section of N_2 molecule.

2.3. XPS measurement

The XPS measurements were made on a VG scientific ESCA Lab II Spectrometer (resolution 0.1 eV) with Mg Kα (1253.6 eV) radiation as the excitation source. The X-ray gun operated at 180 W (12 kV, 15 mA). The spectra were recorded in the fixed analyzer transmission mode, the pass energy being 50 eV. Before the experiments the spectrometer was calibrated against Eb(Au $4f_{7/2}$) = 84.0 eV and Eb(Cu $2p_{3/2}$) = 932.6 eV [29]. The Ti $2p_{3/2}$ or C 1s lines were taken as internal references with a binding energy of 458.5 and 285.0 eV, respectively [29]. An estimated error of +0.1 eV can be assumed for all the measurements. The finely ground oven dried samples were mounted on the standard sample holder and covered by a gold mask. The sample holder was then fixed on a rod attached to the pretreatment chamber. Before transferring them to the main chamber the samples were degassed (1×10^{-7} Torr) in the pretreatment chamber overnight at room temperature. The degassed samples were then transferred into the main chamber and the XPS analysis was done at room temperature and pressures typically less than 10^{-8} Torr. Quantitative analysis of atomic ratios was accomplished by determining the elemental peak areas, following a Shirley background subtraction by the usual procedures, and carried out by adopting the well established procedures in the literature where the sensitivity factors supplied with the instrument were also taken into account [24,29–31].

3. Results and discussion

The N_2 BET surface areas of various supports are presented in Table 1. All the mixed oxide supports prepared in this study are in X-ray amorphous state and exhibited reasonably high BET surface areas. Further, the mixed oxide supports obtained via the homogeneous coprecipitation method are also observed to be uniform throughout the bulk [28,32]. The quantity of MoO_3 required to cover the support surface as a geometrical unimolecular layer can be estimated from theoretical means [33]. Thus, an amount of 0.16 wt.% MoO_3 per m^2 of the support is required in order to cover the support surface as a single lamella of Mo-oxide structure [33]. However, in reality the experimentally observed actual loading was always less than the theoretical estimation and corresponds to about 70% of the theoretical value [13,34–36]. For commercial Degussa P-25 TiO_2, Kim et al. [37] reported the

Table 1
Composition and BET surface areas of the mixed oxide supports used in the present study

Code	Support	Composition of oxides (mole ratio)	BET SA ($m^2\,g^{-1}$)	XRD phases observed
TZ	TiO_2–ZrO_2	1:1	160	Amorphous, $ZrTiO_4$ (trace)
TS	TiO_2–SiO_2	1:1	238	Amorphous, TiO_2-anatase (trace)
TA	TiO_2–Al_2O_3	1:1	159	Amorphous
SZ	SiO_2–ZrO_2	1:1	265	Amorphous
STZ	SiO_2–TiO_2–ZrO_2	1:1:1	330	Amorphous

necessary quantity of MoO_3 as 0.12 wt.% per m^2 of the support. It is an established fact in the literature that the amount of MoO_3 required to form a monolayer on SiO_2 support surface is relatively low because of a weak interaction of the molybdenum ions with the silica support surface. On the other hand, the TiO_2 support takes up more molybdenum per unit surface area than other supports such as Al_2O_3, CeO_2, ZrO_2 and SiO_2 [1,2,7,8,20,21,31,33]. However, in the literature a 12 wt.% of MoO_3 was commonly used for hydroprocessing applications irrespective of the support employed [1,6–8,38]. In view of these reasons a 12 wt.% MoO_3 loading was selected in the present investigation to impregnate on various mixed oxide supports. Further, the pH of the impregnating ammonium molybdate solution was also kept constant (pH = 8) in order to have same molybdenum oxide species on various supports [16]. Very interestingly, none of these catalyst systems exhibited the presence of crystalline MoO_3 from XRD measurements after calcination at 773 K. Further, the oxygen chemisorption measurements made as per the procedure reported elsewhere [38–40] also revealed that the MoO_3 is in highly dispersed state on these mixed oxide supports. The O_2 chemisorption is possible only on the reduced Mo-oxide, which contains the co-ordinately unsaturated sites. This method thus, discriminates between the monolayer and crystalline Mo-oxide phases since their reduction behaviors are entirely different [7,8,38].

The representative XPS bands of Zr 3d, Ti 2p, Si 2p, Al 2p, O 1s and Mo 3d are shown in Figs. 1–6, respectively, and the corresponding binding energies and the full width at half maximum (FWHM) values are summarized in Table 2. For the purpose of better comparison, the XPS bands of Zr 3d, Ti 2p, Si 2p and O 1s pertaining to the supports are shown in Figs. 1a, 2a, 3a and 5a, respectively, and the corresponding bands of MoO_3 containing catalysts synthesized with these supports are shown in Figs. 1b, 2b, 3b and 5b, respectively. These figures and the Table 2 clearly indicate that the XPS bands are highly sensitive to the composition of the mixed oxide support and also the presence of MoO_3 on these carriers.

The binding energy of the Zr $3d_{5/2}$ band in the case of TZ, SZ, STZ mixed oxide samples (Fig. 1a and Table 2) was found to be higher than that of the pure ZrO_2 (182.5 ± 0.1 eV) [41,42]. This shift towards

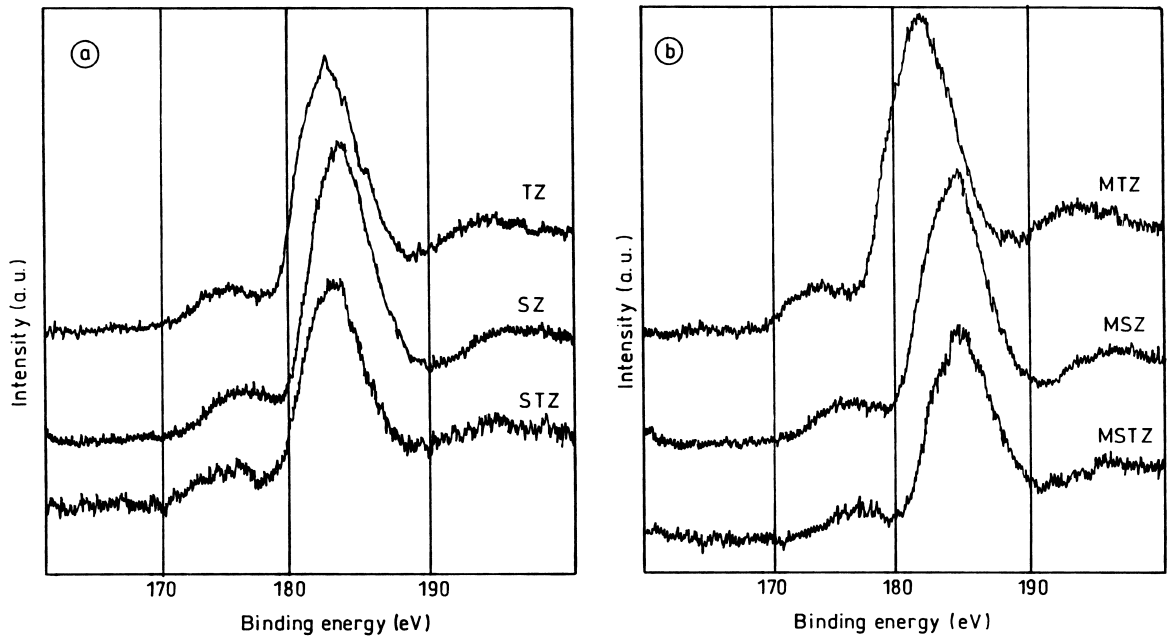

Fig. 1. Zr 3d XPS spectra of various mixed supports and molybdena containing catalysts calcined at 773 K: (a) support; (b) MoO_3/support.

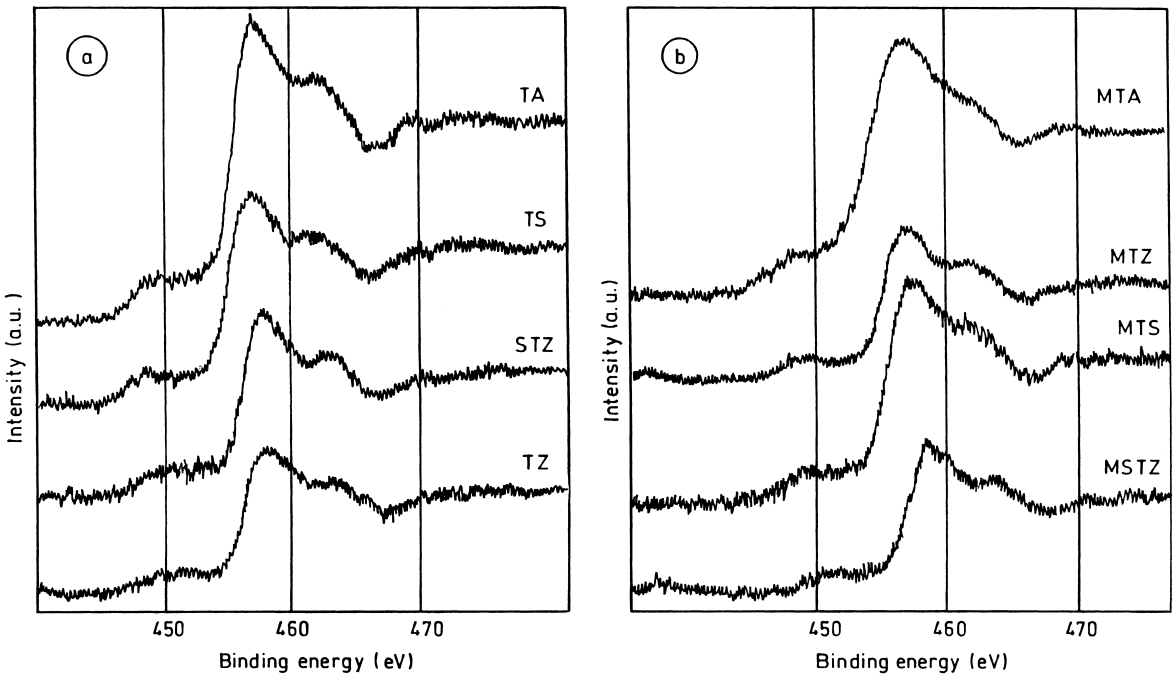

Fig. 2. Ti 2p XPS spectra of various mixed oxide supports and molybdena containing catalysts calcined at 773 K: (a) support; (b) MoO_3/support.

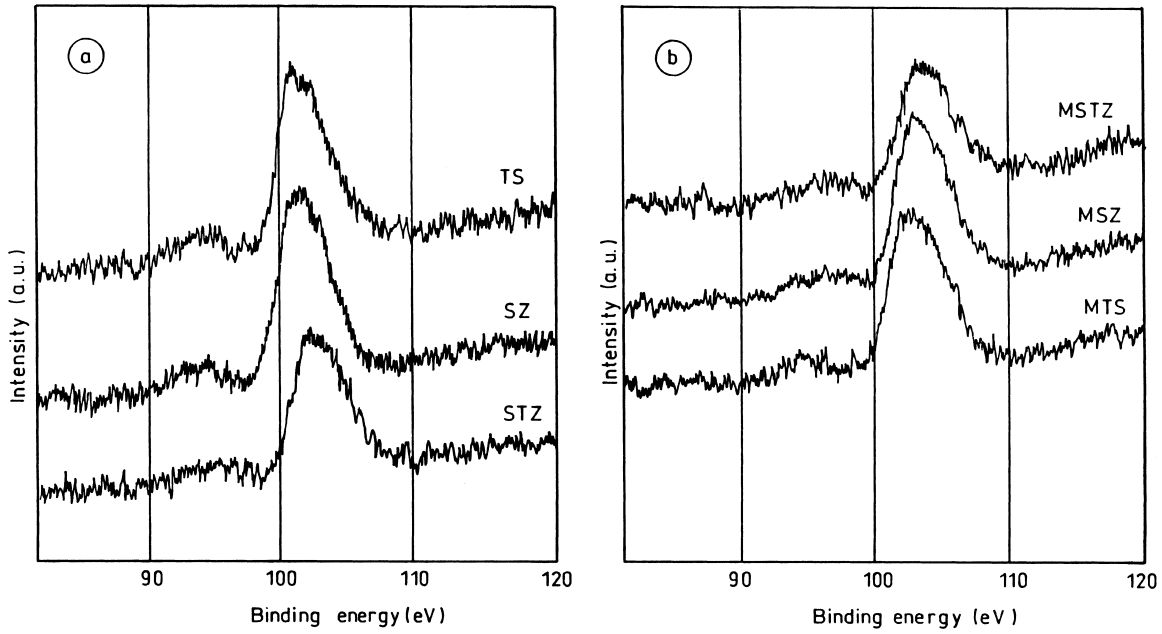

Fig. 3. Si 2p XPS spectra of various mixed oxide supports and molybdena containing catalysts calcined at 773 K: (a) support; (b) MoO_3/support.

higher side could be attributed to an atomic dispersion of zirconia on the other support oxides and/or the change in the coordination number of zirconium by the formation of a Zr–O-Support (TiO_2 or SiO_2) bond. In fact, there is enough evidence in the literature [41,42] in favor of an interaction between zirconia and other oxide supports. In particular, the TiO_2–ZrO_2 combination shows some exceptional properties when compared to that of other combinations. A direct compound formation ($ZrTiO_4$) is observed between TiO_2 and ZrO_2 oxides at 773 K and above temperatures [28]. Other combinations did not exhibit similar behavior. In general, the core-level shifts are assigned to changes in the electronegativities (Pauling term), in the ionicities (Madelung term) and on the final states (relaxation term) in the environment of the photoionized atom [43]. The higher BE as observed in the present study unequivocally indicates that a higher positive charge on the Zr, which implies a higher population of Lewis acid

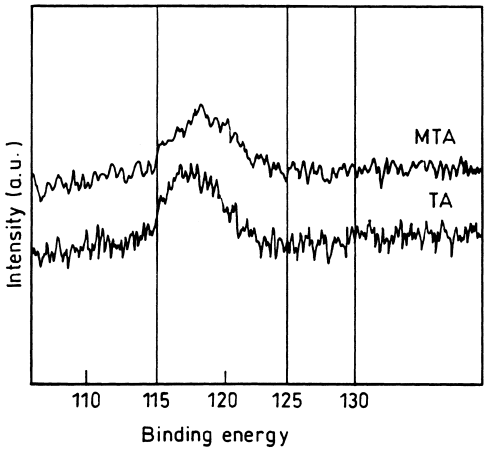

Fig. 4. Al 2s XPS spectra of TiO_2–Al_2O_3 mixed oxide support and MoO_3/TiO_2–Al_2O_3 catalyst calcined at 773 K.

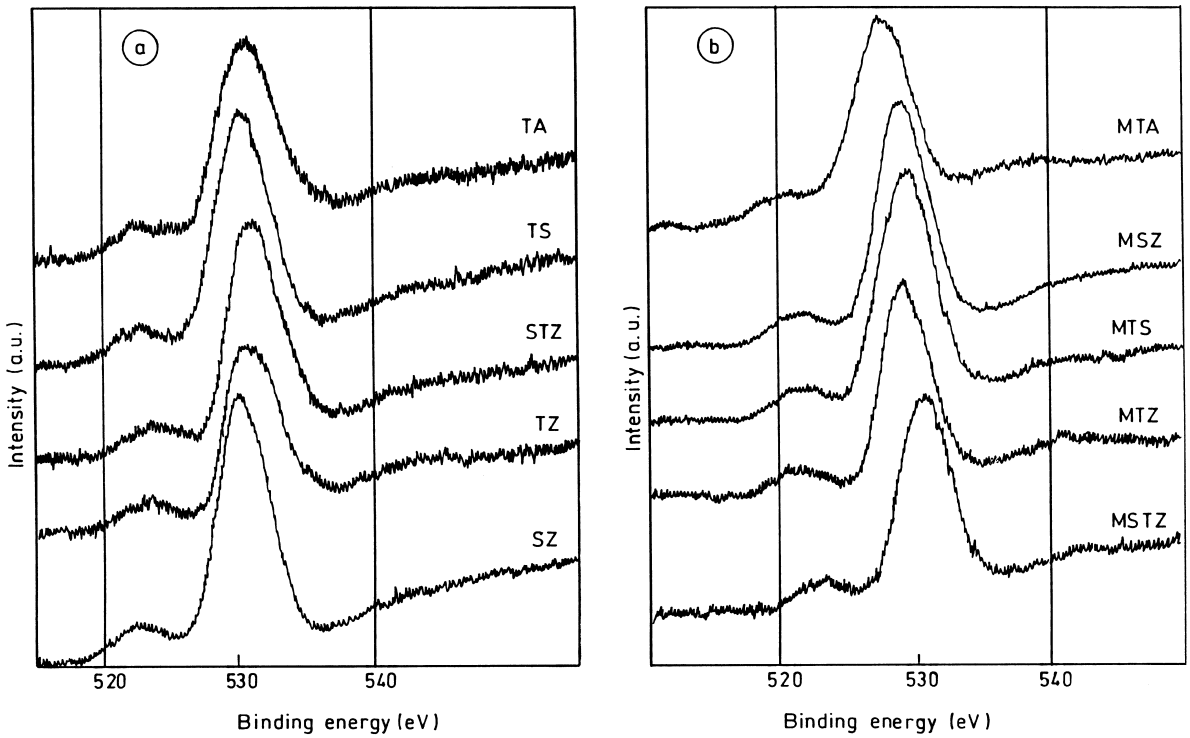

Fig. 5. XPS of the O 1s binding energy region for various mixed oxide supports and molybdena containing catalysts calcined at 773 K: (a) support; (b) MoO_3/support.

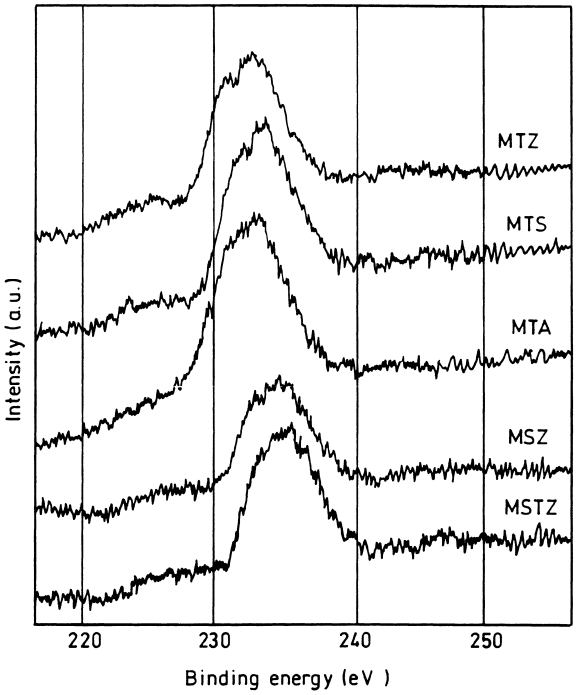

Fig. 6. Mo 3d XPS spectra of various mixed oxide supported MoO_3 catalysts calcined at 773 K.

sites on zirconium when it is in the mixed oxide matrix. Slinkin et al. [44] also reported a similar binding energy shift for a SiO_2–ZrO_2 mixed oxide support. Their study further showed that ionicity of the mixed oxide increases when compared to that of a single oxide. Very recently, Bosman et al. [45] also reported an increase in the binding energy of Zr $3d_{5/2}$ in a differently obtained SiO_2–ZrO_2 mixed oxide sample. The model of Kung [46] envisages that acidity may be generated when differences in electrostatic potential occur for a cation A (oxide stoichiometry AO_y) in a matrix BO_z. If it experiences more negative potential in the matrix BO_z, the electron energy levels of cation A are lower in energy in matrix BO_z and the cation can accept electrons more readily. Due to this the cation A will act as a new Lewis acid site. For oxides having the same stoichiometry, the Kung's model [46] was profitably employed to explain the generation of acidity [45]. The Zr is less electronegative when compared to Ti and Si (Pauling values Zr — 1.4, Ti — 1.5, Si — 1.8), which reflects more ionic character for ZrO_2. The lattice self-potentials (−48.5 eV on average for SiO_2, −42.3 eV for ZrO_2 and −44.7 eV for TiO_2) also indicate that ZrO_2 is more ionic [45]. This means that the Lewis acidity could be predicted when a Zr cation is incorporated in to a more covalent SiO_2 or TiO_2 matrix at the site of the substituting ion. Also the structures proposed by Tanabe et al. [47] and Wu et al. [48] clearly indicate that there is a possibility of the observance of Lewis acid sites on Zr cation when it is in the mixed oxide matrix.

The Ti 2p XPS spectra of Ti containing supports (Fig. 2a) show two shoulder peaks at 458.5 (Ti $2p_{3/2}$) and 464.0 eV (Ti $2p_{1/2}$), respectively, in line with the earlier reports by Wauthoz et al. [49], Mukhopadhyay and Garofalini [50], Wei et al. [51] and Reddy et al. [52]. The observed BE values (Table 2) are in line with the literature reports and are also close to that of pure TiO_2 (458.0–458.5 eV) [29,49–52]. However,

Table 2
XPS binding energies (eV) and FWHM (eV) values of various supports and MoO_3 containing catalysts

Sample	O 1s		Zr 3d		Ti $2p_{3/2}$	Ti $2p_{1/2}$		Si 2p		Al 2s		Mo $3d_{5/2}$	
	BE	FWHM	BE	FWHM	BE	FWHM	BE	BE	FWHM	BE	FWHM	BE	FWHM
TZ	530.5	5.5	184.5	6.5	458.5	6.0	464.0	–	–	–	–	–	–
SZ	529.5	5.5	184.0	6.0	–	–	–	102.5	5.5	–	–	–	–
STZ	531.0	6.0	184.5	6.0	458.5	6.5	465.0	103.0	5.0	–	–	–	–
TS	531.0	6.0	–	–	458.5	7.0	465.3	101.5	5.0	–	–	–	–
TA	531.0	7.0	–	–	459.0	6.0	465.0	–	–	117.5	6.5	–	–
MSZ	530.0	5.5	185.0	6.5	–	–	–	103.5	5.5	–	–	235.0	7.5
MTZ	530.0	5.0	181.0	7.0	458.0	6.5	464.0	–	–	–	–	235.0	7.5
MSTZ	532.0	6.0	185.0	7.0	459.0	7.0	465.5	103.5	5.0	–	–	235.0	7.0
MTS	530.0	6.0	–	–	458.5	7.0	464.0	103.0	6.0	–	–	235.0	7.0
MTA	528.5	6.0	–	–	457.5	8.5	463.0	–	–	118.0	8.5	233.0	8.5

there is a small variation in the case MTA sample, which will be dealt in the latter paragraphs. A similar, however insignificant, variation in the Si 2p BE was also noted for SiO_2 containing TS, SZ and STZ supports (Fig. 3a, Table 2) when compared to that of pure SiO_2 (103.7 eV) [45]. As envisaged by Tanabe et al.[53] that the more dehydroxylation makes the Zr site more positive in the TiO_2–ZrO_2 mixed oxide matrix. A similar analogy can be envisaged for various mixed oxide supports in the present investigation.

The XPS bands of O 1s of various mixed oxide samples are shown in Fig. 4. The O 1s profile is, in general, more complicated due to overlapping contributions of oxygen from individual support oxides as well as from MoO_3 in the case of Mo-containing catalysts. As reported in the literature [29,45,54] the O 1s binding energy for various single oxides SiO_2, ZrO_2, and TiO_2 is 533.0, 530.4, and 530.1 eV, respectively. However, the O 1s band as shown in Fig. 4a and Table 2 for various mixed oxide supports reflects some lowering of the BE for the SZ support and MTA sample. The simultaneous decrease of O 1s and Si 2p BE for the SZ mixed oxide gives an indication of a stronger covalence of Si–O bond in the mixed oxide matrix [45]. Earlier, Barr and Lishka [55] observed an increase in the covalent character of Si–O bonds in Si/Al binary oxide, which normally leads to a large number of Brönsted acid sites. Therefore, generation of some small number of Brönsted acid sites in the case of SZ mixed oxide could be expected since protons are required to balance the excess negative charge on the oxygen atoms. However, the lowering in the binding energies, in the case of MTA sample, may be due to the formation of a molybdate compound [$Al_2(MoO_4)_3$] between MoO_3 and Al_2O_3, which reorganizes the uniformity in the composition of TiO_2–Al_2O_3 oxide.

The influence of MoO_3 on various mixed oxides is emphasized in the following paragraphs. As can be noted from Table 2 that there is a significant fall in the BE of Zr 3d core level electrons in the case of MTZ sample. However, no such decrease is observed in the case of Ti 2p lines for this sample. As the electron deficiency is more on Zr site so it is obvious that there will be a co-ordination by Mo–O-terminal of the MoO_3. Hydroxyl groups are normally present more on titania rich domain and co-ordinate through Ti–O-terminal to the Mo center of the MoO_3 as shown in Scheme 1. This type of bi-dentate species formation

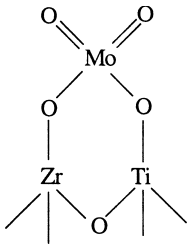

Scheme 1.

has been reported recently by Rajagopal et al. [56], and Henker et al. [57] for MoO_3/Al_2O_3–SiO_2 catalyst system. According to them, at low loadings molybdate reacts strongly by forming bidentate species with a pair of adjacent surface hydroxyl groups of the support. However, at higher loadings (near or above monolayer coverage) anchoring of molybdate anions by reacting with a hydroxyl and an adjacent Al-cus (coordinately unsaturated site) has been proposed. The structure proposed by Ramirez and Gutierrez-Alejandre [58] for WO_3/TiO_2–Al_2O_3 system recently also strengthens this speculation. Thus, there will be a decrease in both Lewis and Brönsted acid site concentration after doping with MoO_3. As can be seen from Table 2 that there is a small increase in the FWHM of Zr 3d peak in the case Mo-containing samples (MSZ, MTZ and MSTZ) when compared to that of pure supports. The broadening of Zr 3d peak indicates an electronic interaction between the active component MoO_3 and the support oxide, in particular the ZrO_2. A definite compound formation ($ZrMo_2O_8$) was also noted between MoO_3 and ZrO_2 beyond 773 K calcination temperatures [28]. In the case of SZ and STZ supports, the Si 2p and Ti 2p BE values have been shifted to higher side after doping with MoO_3, which indicate a lowering of negative charge density on Si and Ti atoms due to the binding through M–O– (where M is either Si or Ti) terminal to the molybdenum.

A closer examination at the binding energy profiles of Si 2p, Ti 2p, Al 2s and O 1s lines (Table 2) for the TS and TA supports before and after Mo doping provides an interesting information. The O 1s BE of the TS (531.0 eV) support was found to shift to a lower value when compared to that of pure SiO_2 (533.0 eV). Since the Ti is more electropositive in nature than the Si, the O 1s core electron binding

energy is decreased when a Si–O–Si bond is replaced by a Ti–O–Si bond in the TS mixed oxide matrix. The Ti–O bond is more ionic in character thus making Si–O bond more covalent by increasing the negative charge density on oxygen atom due to which the O 1s BE has been shifted to the lower side. The decrease in Si 2p BE in the case of TiO_2–SiO_2 mixed oxide support compared to that of pure SiO_2 also establishes the more covalent nature of Si–O bond in TS mixed oxide. This observation is in line with our earlier XPS study of the V_2O_5/TiO_2–SiO_2 catalyst system [52] and also the reports made by some other groups [53]. There is also a shift of Si 2p BE towards higher value after molybdena doping on STZ, TS and SZ supports, which implies a partial removal of negative charge density from Si atom due to bonding through Si–O– terminals. Presence of Brönsted acid sites on Si in TS mixed oxide are mainly due to more strength of Si–OH bonds because of charge imbalance created between octahedral Ti and tetrahedral Si [59].

The XPS spectra of TA and MTA samples (Fig. 4) reveals some interesting information. The Al 2s line for both TA and MTA samples shifted to the lower side when compared to that of pure γ-Al_2O_3 (119.1 eV) [60]. The shift of the Al 2s peak towards lower side in both TA and MTA samples gives indication about changes in the electronic environment around Al atom in both the cases. Incorporation of Al^{3+} cation into TiO_2 matrix causes an increase in the negative charge in the vicinity of Al^{3+} surroundings because of excess oxygen around it. This effect is thus reflected in the decrease of Al 2s BE. The excess negative charge may be balanced by adsorption of protons on the surface and which may act as new Brönsted acid sites. Bonding through Al–O– terminal to MoO_3 minimizes the excess negative charge around Al^{3+} cation due to which a little increase in the Al 2s BE is noted in the MTA sample when compared to that of TA support.

A closer examination of Mo 3d bands and FWHM values as shown in Fig. 6 and Table 2 provide an interesting information about the oxidation state and chemical nature of molybdena species on various supports. The binding energy values presented in Table 2 indicate the presence of Mo(VI) species on all the support surfaces [25]. Very interestingly, the Mo 3d doublet is well resolved in the case of MTZ and MTS samples. Among all the samples the peak broadening is maximum in the case of MTA sample which has the highest FWHM value of 8.5 eV. Nag [21] studied the interaction of molybdena with different single oxide supports by XPS technique. It was noted that the resolution of the doublet peak was quite poor for MoO_3/Al_2O_3 catalyst and improved considerably as one passes from Mo/SiO_2 to Mo/ZrO_2 to Mo/TiO_2 systems. The broadening of ESCA peak has been attributed to various factors including (1) the presence of more than one type of Mo(VI) with different chemical characteristics which cannot be discerned by ESCA [23], (2) electron transfer between active component and the support (metal-support interaction). The previous characterization studies using in situ Raman and XANES spectroscopies revealed that the structure of surface molybdenum oxide species are primarily isolated, tetrahedrally coordinated at lower loadings and tend towards polymerized, octahedrally coordinated at higher loadings (near or above monolayer coverage) [4]. At monolayer coverage the structure of surface molybdenum oxide species primarily possesses an octahedral coordination on TiO_2 and mixture of tetrahedral and octahedral coordination on Al_2O_3. The ionic radii of Al^{3+} and Mo^{6+} in the tetrahedral (0.39 and 0.41 Å) and octahedral (0.535 and 0.59 Å) configuration, respectively, are similar. Cacers et al. [61] suggested that there would be more homogeneous distribution of Mo species on TiO_2 than on Al_2O_3. The maximum Mo 3d peak broadening in the case of MTA sample provides evidence regarding the existence of different octahedral and tetrahedral Mo species on TA mixed oxide surface. The size of Mo^{6+} also resembles more with ZrO_2 making a uniform distribution of MoO_3 species on ZrO_2 support [62]. Thus, on the TZ and TS supports the Mo^{6+} species has more uniform chemical environment than on the TA support. This fact is clearly reflected in the better resolution of spin–orbit coupled peaks in Mo 3d photoelectron spectra. Formation of $ZrMo_2O_8$ compound at higher temperature (973 K) for MTZ system due to better fittings of Mo^{6+} in ZrO_2 matrix has been observed recently [63].

The dispersion of metals or metal oxides on various support surfaces can be estimated from ESCA atomic intensity ratio measurements of different peaks [24,52,60,64–66]. A detailed account of these calculations have been elaborated elsewhere [24]. As mentioned earlier, the impregnated molybdenum oxide is in a highly dispersed state and expected to be

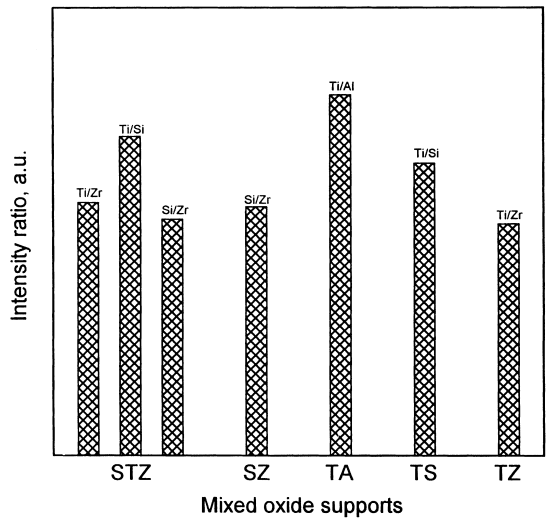

Fig. 7. XPS intensity ratios for various mixed oxide supports.

uniformly distributed on various supports. The dispersion measurements obtained from XPS atomic intensity ratios are expected to provide information about the relative dispersion of Mo on various supports. Thus, obtained atomic ratios for various mixed oxide supports and Mo-containing catalysts are shown in Figs. 7 and 8, respectively. As can be noted from Fig. 7 that the Ti:Al ratio is maximum among all the intensity ratios calculated. This observation gives an impression that in the case of TA support the surface is more enriched with TiO_2. A similar high surface enrichment of TiO_2 can also be noted in the case of TS and STZ supports. However, in the case of TZ and SZ supports the distribution of individual oxides is more uniform on the surface. As can be noted from Fig. 8 that the Mo:Al ratio has been found to be maximum when compared to other corresponding intensity ratios indicating a high dispersion of molybdena on Al_2O_3 in the case of TA mixed oxide support. This clearly indicates that the interaction between MoO_3 and Al_2O_3 is more when compared to other oxides [47]. Of course, the formation of a $Al_2(MoO_4)_3$ compound is a well established fact in the literature in the case of MoO_3/Al_2O_3 catalysts when calcined at 773 K. Further, the Mo:Ti and Mo:Si intensity ratios in the case of MTS catalyst give an impression that the dispersion of molybdena is more on Si than on Ti. A closer comparison of the Ti:Si ratio for TS and MTS catalysts show that the surface enrichment of Ti^{4+} is more when compared to that of Si^{4+}, thus making the IMo/ITi value lower. However, the Mo:Ti and Mo:Zr ratios in the case of MTZ and MSTZ samples show that the Ti^{4+} and Zr^{4+} both contribute almost equally in the dispersion of molybdena on these corresponding mixed oxides.

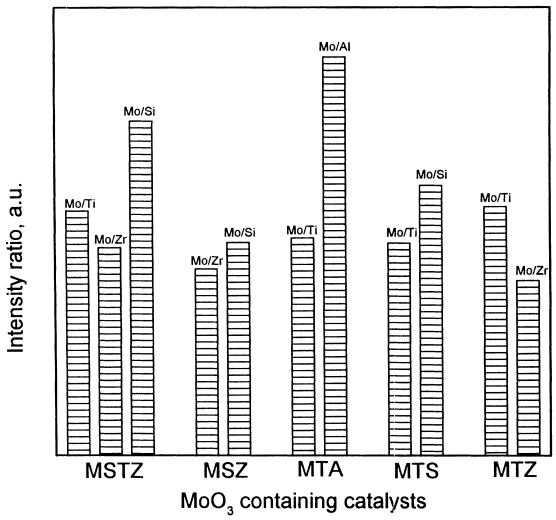

Fig. 8. XPS intensity ratios for various mixed oxide supported MoO_3 catalysts.

4. Conclusions

The XPS characterization of MoO_3 on TiO_2–ZrO_2, TiO_2–SiO_2, TiO_2–Al_2O_3, SiO_2–ZrO_2, and SiO_2–TiO_2–ZrO_2 mixed oxides provides some valuable information. Among various mixed oxide catalysts studied the MTZ and MTA have drawn special attention. The shift in Zr 3d XPS binding energy towards lower value after doping the TZ with MoO_3 indicates more negative charge density on zirconium. Similarly, the Ti site also acquires more negative charge density when molybdenum is anchored on TA mixed oxide surface. The atomic intensity ratio measurements give an impression that the molybdena dispersion is more on Al_2O_3 domain than on TiO_2 in the case of TA mixed oxide support. The maximum broadening of Mo 3d as observed from FWHM values also indicates that the presence of different Mo(VI) species on the

TA support. On the other hand, the better resolution of Mo 3d doublet peaks in the case of MTZ and MTS catalysts shows a homogeneous distribution of Mo(VI) species on the TZ and TS support surfaces. The core electron BE of all the elements in the mixed oxides investigated have shifted either to lower or higher side depending on the lattice potential of the constituent oxide matrices. Kung's model [46] has been found to be more pragmatic in explaining the observed BE shifts due to variation in lattice potential.

Some of these mixed oxide supports investigated are highly promising for the dispersion of molybdenum oxide and exploiting them for various commercially important reactions such as hydroprocessing. Further studies are under active progress to assess the activity and selectivity of these catalysts in relation to the population of Lewis and Brönsted acid sites.

Acknowledgements

Thanks are due to University Grants Commission, New Delhi, for the award of a senior research fellowship to BC.

References

[1] F.E. Massoth, Adv. Catal. 27 (1978) 265.
[2] J. Haber, The Role of Molybdenum in Catalysis, Climax Molybdenum Co., Ann Arbor, MI, 1981.
[3] B.C. Gates, J.R. Katzer, G.C.A. Schuit, Chemistry of Catalytic Processes, McGraw-Hill, New York, 1979 (Chapter 5).
[4] H. Hu, I.E. Wachs, J. Phys. Chem. 99 (1995) 10911, and references therein.
[5] H. Knözinger, E. Taglauer, Catal. Roy. Soc. Chem., Cambridge 10 (1993) 1.
[6] W. Zhaobin, X. Quin, G. Xiexian, P. Grange, B. Delmon, Appl. Catal. 75 (1991) 179.
[7] B.M. Reddy, V.S. Subrahmanyam, Appl. Catal. 27 (1986) 1.
[8] B.M. Reddy, K.V.R. Chary, B.R. Rao, V.S. Subrahmanyam, C.S. Sunandana, N.K. Nag, Polyhedron 5 (1986) 191.
[9] L. Wang, W.K. Hall, J. Catal. 66 (1980) 251.
[10] J. Fung, I. Wang, J. Catal. 130 (1991) 577.
[11] H. Hattori, M. Itoh, K. Tanabe, J. Catal. 38 (1975) 172.
[12] H.J.M. Bosman, E.C. Kruissink, J.V. Spoel, F.V. Brink, J. Catal. 148 (1994) 660.
[13] A. Baiker, P. Dollenmeier, M. Glinski, A. Reller, Appl. Catal. 35 (1987) 365.
[14] P.G. Smirniotis, M.A. Abraham, Catal. Today (Special Issue), 1998, p. 40.
[15] P. Ratnasamy, S. Sivasanker, Catal. Rev. Sci. Eng. 22 (1980) 401.
[16] H. Knözinger, in: M.J. Phillips, M. Ternan (Eds.), Proceedings of the 9th International Congress on Catalysis, Vol. 5, Calgary, 1988, Chem. Institute of Canada, Ottawa, p. 20.
[17] A.N. Startsev, Catal. Rev. Sci. Eng. 37 (1995) 353, and references therein.
[18] E. Taglawer, W. Heiland, Appl. Phys. 9 (1976) 261.
[19] D.S. Zingg, L.E. Markovsky, R.E. Tischer, F.R. Brown, D.M. Hercules, J. Phys. Chem. 84 (1980) 2898.
[20] F.E. Massoth, G. Murlidhar, J. Shabtai, J. Catal. 88 (1984) 53.
[21] N.K. Nag, J. Phys. Chem. 91 (1987) 2324, and references therein.
[22] A.W. Armour, P.C.H. Mitchell, B. Folkesson, R. Larson, J. Less Common Met. 36 (1974) 361.
[23] P. Ratnasamy, J. Catal. 40 (1975) 137.
[24] Y. Okamoto, T. Imanaka, S. Teranishi, J. Phys. Chem. 85 (1981) 3798.
[25] T.A. Patterson, J.C. Carver, D.E. Leyden, D.M. Hercules, J. Phys. Chem. 80 (1976) 1700.
[26] T. Edmonds, P.C.H. Mitchell, J. Catal. 64 (1980) 431.
[27] G. Mestl, N.F.D. Verbruggen, F.C. Lange, B. Tesche, H. Knözinger, Langmuir 12 (1996) 1817, and references therein.
[28] B.M. Reddy, B. Manohar, S. Mehdi, J. Solid State Chem. 97 (1992) 233.
[29] D. Briggs, M.P. Seah (Eds.), Practical Surface Analysis, Auger and X-ray Photoelectron Spectroscopy, 2nd Edition, Vol. 1, Wiley, New York, 1990.
[30] A. Savitzky, M.J.E. Golay, Anal. Chem. 36 (1964) 1627.
[31] D.A. Shirley, Phys. Rev. B 5 (1972) 4709.
[32] C.U.I. Odenbrand, P.L.T. Gabrielsson, J.G.M. Brandin, L.A.H. Andersson, Appl. Catal. 78 (1991) 109.
[33] A.J. Van Hengstun, J.G. Van Ommen, H. Bosch, P.J. Gellings, Appl. Catal. 5 (1983) 207.
[34] G.C. Bond, J. Perez Zurtia, S. Flamrez, P.J. Gellings, H. Bosch, J.G. Van Ommen, B.K. Kip, Appl. Catal. 22 (1986) 361.
[35] B.M. Reddy, E.P. Reddy, S.T. Srinivas, V.M. Mastikhin, A.V. Nosov, O.B. Lapina, J. Phys. Chem. 96 (1992) 7076.
[36] J. Haber, A. Kozlowska, R. Kozlowski, J. Catal. 102 (1986) 52.
[37] D.S. Kim, Y. Kurusu, I.E. Wachs, F.D. Hardcastle, K. Segawa, J. Catal. 120 (1989) 325.
[38] B.M. Reddy, K.V.R. Chary, V.S. Subrahmanyam, N.K. Nag, J. Chem. Soc., Faraday Trans. 81 (1985) 1655.
[39] B.M. Reddy, B. Manohar, E.P. Reddy, Langmuir 9 (1993) 1781.
[40] B.M. Reddy, K.S.P. Rao, V.M. Mastikhin, J. Catal. 113 (1988) 556.
[41] W.M. Mullins, B.L. Averbach, Surf. Sci. 206 (1988) 29.
[42] D.A. Stephenson, N.J. Binkowski, J. Non Cryst. Solids 22 (1976) 399.
[43] A. Jimenez-Gonzalez, D. Schmeisser, J. Catal. 130 (1991) 332.
[44] A.A. Slinkin, A.L. Klyachko, E. Shpiro, G.I. Kapustin, T.N. Kucherova, A.Yu. Stakheev, L.V. Ermolov, Kinet. Katal. 32 (1991) 725.
[45] H.J.M. Bosman, A.P. Pijpers, A.W.M.A. Jaspers, J. Catal. 161 (1996) 551.

[46] H.H. Kung, J. Solid State Chem. 52 (1984) 191.
[47] K. Tanbe, M. Misono, Y. Ono, H. Hattori, Stud. Surf. Sci. Catal. 51 (1989) 1.
[48] J.-C. Wu, S.C. Chung, A.Y. Ching-Lan, I. Wang, J. Catal. 87 (1984) 98.
[49] P. Wauthoz, M. Ruwet, T. Machej, P. Grange, Appl. Catal. 69 (1991) 149.
[50] S. Mukhopadhyay, S. Garofalini, J. Non-Cryst. Solids 126 (1990) 202.
[51] Z. Wei, Q. Xin, X. Guo, E.L. Sham, P. Grange, B. Delmon, Appl. Catal. 63 (1990) 305.
[52] B.M. Reddy, I. Ganesh, E.P. Reddy, J. Phys. Chem. B 101 (1997) 1769.
[53] K. Tanabe, T. Sumiyoshi, K. Shibata, Bull. Chem. Soc. Jpn. 47 (1974) 1064.
[54] R. Castillo, B. Koch, P. Ruiz, B. Delmon, J. Catal. 161 (1996) 524.
[55] T.L. Barr, M.A. Liska, J. Am. Chem. Soc. 108 (1986) 3178.
[56] S. Rajagopal, J.A. Marzari, R. Miranda, J. Catal. 151 (1995) 192.
[57] M. Henker, K.P. Wendlandt, J. Valyon, R. Bornmann, Appl. Catal. 69 (1991) 205.
[58] J. Ramirez, A. Gutierrez-Alejandre, J. Catal. 170 (1997) 102.
[59] Z. Liu, J. Tabora, R.J. Davis, J. Catal. 149 (1994) 117.
[60] Y. Okamoto, H. Tomioka, Y. Katoh, T. Imanaka, S. Teranishi, J. Phys. Chem. 84 (1980) 1833.
[61] C.V. Caceres, J.L.G. Fierro, J. Lazaro, A.L. Agudo, J. Soria, J. Catal. 122 (1990) 113.
[62] T. Ono, H. Kamisuki, H. Hisashi, H. Miyata, J. Catal. 116 (1989) 303.
[63] B.M. Reddy, B. Chowdhury, J. Catal. 179 (1998) 413.
[64] D. Briggs, J. Electron Spectrosc. Relat. Phenomenon 9 (1976) 487.
[65] J.S. Brinen, J.L. Schmitt, J. Catal. 45 (1976) 274.
[66] B.M. Reddy, B. Chowdhury, I. Ganesh, E.P. Reddy, T.C. Rojas, A. Fernández, J. Phys. Chem. B 102 (1998) 10176.